Asia-Pac. J. Atmos. Sci., 54(1), 43-52, 2018
DOI:DOI:10.1007/s13143-017-0058-8
pISSN 1976-7633 / eISSN 1976-7951

On the Angular Momentum Loss of Tropical Cyclones: An *f*-Plane Approximation

Hyun-Gyu Kang[1,2], Hyeong-Bin Cheong[1], and Won-Ho Kim[1]

[1]*Department of Environmental Atmospheric Sciences, Pukyong National University, Busan, Korea*
[2]*BK21 Plus Project of the Graduate School of Earth Environmental Hazard System, Busan, Korea*

(Manuscript received 4 October 2016; accepted 11 May 2017)

Abstract: The angular momentum for ideal axisymmetric tropical cyclones on the *f*-plane is investigated with a focus on the total-volume integrated quantity. Budget analysis of the momentum equation at cylindrical coordinates shows that a tropical cyclone loses angular momentum during its development and mature stages due to the dynamical difference between the viscous inward-flow near the surface and the angular momentum conserving outward-flow aloft. The total relative angular momentum of a tropical cyclone, as a result, can be negative (i.e., implying anticyclonic rotation as a whole) despite intense cyclonic wind in the tropospheric layers. This anticyclonic rotation was measured in terms of the super-rotation ratio, the ratio of total relative angular momentum to the planetary angular momentum. Simulations with the numerical model of Weather Research and Forecasting (WRF) version 3.4.1 was found to be in favor of the theoretical angular-momentum budget analysis. It was revealed in the numerical simulations that the super-rotation ratio was negative, indicating a sub-rotation, as was predicted by analysis. The sub-rotation ratio was found to be less than one percent for typical tropical cyclones. To show the angular momentum decrease even in the decaying stage, numerical simulations where the thermal forcing by sea surface temperature switched off in the mature stage were carried out. In support of the angular momentum budget analysis, the results indicated that the angular momentum also decreases for a while soon after the forcing was eliminated.

Key words: Tropical cyclone, angular momentum, surface friction, super- or sub-rotation, cyclonic or anticyclonic rotation

1. Introduction

Tropical cyclone is a low-pressure vortical flow that is generated over low-latitude warm oceans and is accompanied by heavy rainfall and strong winds (Anthes, 1982). A well-developed tropical cyclone consists of a nearly-symmetric azimuthal flow (or tangential flow) and a vertical-radial circulation, which are often referred to as the primary circulation and secondary circulation, respectively (Anthes, 1982; Holland, 1983; Kwon and Cheong, 2010; Hakim, 2011). The vertical-radial flow is a thermally-driven direct circulation, whereas the azimuthal flow is established as a result of the angular momentum conservation associated with the radial motion of direct circulation. The constraint of angular momentum conservation helps the inward motion to achieve cyclonic (or counterclockwise) rotation in the northern hemisphere. In the upper part of the tropical cyclone, where outward motion (or divergent flow) is maintained, the anticyclonic flow is formed by the same angular momentum constraint (Pielke, 1984; Montgomery et al., 2001; Kwon and Cheong, 2010; Persing et al., 2013). The angular momentum, however, is less conserved in the boundary layer than in the upper outflow region due to turbulence friction. This was illustrated by Emanuel (2003) using a simple tropical cyclone schematic structure. Therefore, once the tropical cyclone is formed, the angular momentum is destined to decrease monotonically with time. The extent to which the angular momentum (i.e., the angular momentum deficit due to friction) is lost depends on the surface condition and may be sensitive to the detailed flow structure. However, it is known that the angular momentum, if measured within the domain of a small radius from the center, should increase during development (Anthes, 1982; Holland, 1983; Pielke, 1984; Emanuel, 2003). Considering that a tropical cyclone develops due to the presence of outflow aloft, which typically extends horizontally to a couple of thousand kilometers away from the center (e.g., Anthes, 1982; Kwon and Cheong, 2010), it may be necessary to deal with the tropical cyclone as a system inclusive of the circulations within a few thousands kilometers in order to better understand the dynamical features. In such a system the total angular momentum integrated over a large volume of air provides insights which are useful to understand the dynamics of tropical cyclone. By investigating the total angular momentum and its budget, it is also possible to quantify the change of total angular momentum of the system and the transport of angular momentum at lateral boundaries of tropical cyclone for a given radius and height.

The angular momentum loss has previously been vividly demonstrated in an equilibrium-state axisymmetric storm that developed from the rest state tropical atmosphere (Hakim, 2011). The isolines of angular momentum, which align vertically at an initial state of no motion, are moved away from the storm center in the outward radial flow region. Deformation of angular momentum contours accompanied by the radial-vertical motion is found more conspicuously in the

Corresponding Author: Hyeong-Bin Cheong, Department of Environmental Atmospheric Sciences, Pukyong National University, Yongso-ro 45, Namgu, Busan 48513, Korea.
E-mail: hbcheong@pknu.ac.kr

outward-motion region than it is in the inward-motion region. That is, along the trajectory of an air parcel on the radial-vertical cross section, the angular momentum is better conserved in the upper region of outward motion (Tuleya and Kurihara, 1974; Anthes, 1982; Hakim, 2011) than it is in the lower region. Due to the difference in the angular momentum conservation in the upper and lower layers, tropical cyclone, as a whole, tends to have negative relative angular momentum (RAM). Such a circulation system is often termed a sub-rotation, which is typical of a positive-buoyancy driven circulation in a rotating fluid. The opposite circulation system is termed a super-rotation, which is typical of negative-buoyancy driven circulation (Hignett et al., 1981; Read, 1986; Kimura et al., 1992).

In this study, the angular momentum of an ideal tropical cyclone having an axisymmetric structure and incorporating an *f*-plane approximation (Montgomery et al., 2001; Persing et al., 2013; Montgomery et al., 2015) is investigated. A simple analysis of the momentum equation is provided to give an insight into the angular momentum conservation of axisymmetric tropical cyclones. Then, numerical simulations are performed to support this analysis using the state-of-the-art numerical model WRF v3.4.1 (Skamarock et al., 2008). As initial conditions of the simulation, two types of the axisymmetric tropical cyclone are incorporated: one with a realistic boundary layer structure and the other without. The paper is organized as follows. The next section presents the angular momentum budget of an ideal axisymmetric tropical cyclone on the polar coordinate system. Section 3 is devoted to numerical simulation of an ideal axisymmetric tropical cyclone using WRF v3.4.1. The final section presents the summary and concluding remarks.

2. Angular momentum loss of tropical cyclones

a. Angular momentum conservation equation

The azimuthal momentum equation of a rotating atmosphere in cylindrical coordinates is given as (Bird et al., 2007; Persing et al., 2013)

$$\rho\left(\frac{\partial v}{\partial t}+u\frac{\partial v}{\partial r}+\frac{v}{r}\frac{\partial v}{\partial \lambda}+w\frac{\partial v}{\partial z}+\frac{uv}{r}+fu\right)=-\frac{1}{r}\frac{\partial p}{\partial \lambda}+D_v, \tag{1}$$

where ρ is the density of air, t is time, u, v, and w imply radial (r), azimuthal (λ), and vertical (z) velocity, respectively, $f[\equiv 2\Omega\sin\theta_0]$ is the Coriolis parameter for a rotating plane with the angular velocity Ω at the latitude θ_0, p denotes pressure, and D_v represents the friction [or subgrid-scale diffusive and planetary boundary layer tendency (see Persing et al., 2013)]:

$$D_v=\frac{1}{r^2}\frac{\partial}{\partial r}r^2\rho_0\tau_r+\frac{1}{r^2}\frac{\partial}{\partial \lambda}\rho_0\tau_\lambda+\frac{\partial}{\partial z}\rho_0\tau_z, \tag{2}$$

where τ_r, τ_λ and τ_z are (subgrid-scale turbulent or eddy) momentum fluxes of the radial, azimuthal, and vertical direction, respectively, and $\rho_0(z)$ is the basic state horizontally-averaged density (Persing et al., 2013). Combined with the continuity equation,

$$\frac{\partial \rho}{\partial t}+\frac{1}{r}\left(\frac{\partial}{\partial r}\rho ru+\frac{1}{r}\frac{\partial}{\partial \lambda}\rho rv+\frac{\partial}{\partial z}\rho rw\right)=0, \tag{3}$$

the absolute angular momentum equation is obtained:

$$\frac{\partial M_a}{\partial t}+\nabla_F\cdot(rM_a\mathbf{v})=-\frac{\partial p}{\partial \lambda}+rD_v, \tag{4}$$

where $\mathbf{v}[\equiv(u, v, w)]$ is the velocity vector (the dot indicates the inner product), and

$$\begin{aligned} &M_a=M_r+M_\Omega\equiv\rho rv+\frac{1}{2}\rho fr^2 \\ &\nabla_F\equiv\frac{1}{r}\left(\mathbf{r}\frac{\partial}{\partial r}+\boldsymbol{\lambda}\frac{1}{r}\frac{\partial}{\partial \lambda}+\mathbf{z}\frac{\partial}{\partial z}\right) \end{aligned}, \tag{5}$$

with the bold-faced variables meaning the unit vectors. Integrating Eq. (4) over a cylindrical column of air of $0\le r\le R$ and $0\le z\le H$ gives

$$\begin{aligned} \frac{d\hat{M}_a}{dt}&\equiv\frac{d\hat{M}_r}{dt}+\frac{d\hat{M}_\Omega}{dt} \\ &=-\int_0^H[\langle ruM_a\rangle]_{r=R}\,dz+\int_0^H\int_0^R\langle rD_v\rangle rdrdz \\ \hat{M}_r&=\int_0^H\int_0^R\langle M_r\rangle rdrdz \\ \hat{M}_\Omega&=\int_0^H\int_0^R\langle M_\Omega\rangle rdrdz \end{aligned}, \tag{6}$$

where the bracket denotes azimuthal integration, i.e., $\langle\otimes\rangle\equiv\int_0^{2\pi}\otimes d\lambda$, and $\hat{M}_a$ indicates the total absolute angular momentum (TAAM) on a rotating plane. The radius and height, R and H, can be taken arbitrarily, but will be given as large as those of a typical tropical cyclone. Equation (6) states that in the TAAM, $\hat{M}_a$ is conserved in the absence of torques such as radial-advective flux and friction, as represented on the right hand side. To a first approximation, the total planetary angular momentum (TPAM; $\hat{M}_\Omega$) remains unchanged if the integration is performed over thousands of kilometers from the center (as in this study), and it is exactly conserved for motions with a constant density. Therefore, it may be written that $d\hat{M}_a/dt \rightarrow d\hat{M}_r/dt$.

b. Frictional torque and the angular momentum loss of a tropical cyclone

The azimuthal-averaged friction term can be divided into radial and vertical components (Persing et al., 2013):

$$\langle D_v\rangle=\frac{1}{r^2}\frac{\partial}{\partial r}\rho_0r^2\langle\tau_r\rangle+\frac{\partial}{\partial z}\rho_0\langle\tau_z\rangle. \tag{7}$$

According to the scale analysis by Vogl and Smith (2009), the radial momentum flux (the first term) is $O(10^{-3})$ times smaller than the vertical momentum flux (the second term). Since the scale for the radial friction is inversely proportional to the radial scale, this difference would increase as the radial

distance of integration increases. In this study, we focused on the large system of a tropical cyclone rather than on the inner core region. Therefore, the first term on the right hand side of Eq. (7) is small enough to be neglected. Graphical evidence for this can also be found in Persing et al. (2013; see their Figs. 10 e-f). The conservation equation of total relative angular momentum (TRAM; $\hat{M}_r$) of Eq. (6) is then rewritten as

$$\frac{d\hat{M}_r}{dt} = N_r + N_{zH} + N_{zB}, \tag{8}$$

where N_r is the torque due to the radial-advective momentum flux, and N_{zH} and N_{zB} are the torques associated with the top- and surface-frictional momentum fluxes, respectively:

$$\begin{aligned} N_r &= -\int_0^H [\langle ruM_r \rangle]_{r=R} dz \\ N_{zH} &= +\int_0^R \rho_H r^2 \langle \tau_{zH} \rangle dr \\ N_{zB} &= -\int_0^R \rho_s r^2 \langle \tau_{zB} \rangle dr, \\ [\rho_H &= \rho_0(z_H),\ \rho_s = \rho_0(z_s)] \end{aligned} \tag{9}$$

with τ_{zH} and τ_{zB} denoting the vertical eddy momentum flux (or viscous flux of momentum) at the top and the surface, respectively. Equation (8) can be considered as a fluid motion counterpart of the relationship between the net torque and angular momentum of a rotating body (e.g., Symon, 1971). Similar to this, but from the Lagrangian point of view following air-parcel motion, such a relationship was illustrated by Emanuel (2003) for the axisymmetric circulations in a tropical cyclone. If the radius R of integration is taken to be large enough for the radial velocity to vanish, it holds that $N_r = 0$, then, in this case the time change of TRAM ($\hat{M}_r$) is only subject to the momentum flux at vertical boundaries.

Dealing with the momentum fluxes such as τ_r, τ_λ and τ_z, associated with the friction of atmospheric motion, is a challenging problem. It is expressed in many ways under different approximations and assumptions. Widely accepted formulas for this purpose are to represent them by means of K-theory (see Holton and Hakim, 2012, their Eq. (8.27); Persing et al., 2013; Montgomery and Smith, 2017):

$$\begin{aligned} \langle \tau_{zH} \rangle &= K_m \frac{\partial \langle v \rangle}{\partial z} \text{ at } z = H \\ \langle \tau_{zB} \rangle &= K_m \frac{\partial \langle v \rangle}{\partial z} = \begin{cases} +u_*^2 \text{ for cyclonic flow at } z_s \\ -u_*^2 \text{ for anticyclonic flow at } z_s \end{cases}, \end{aligned} \tag{10}$$

where K_m and z_s are the vertical eddy viscosity and surface-layer height, respectively, and u_* represents the friction velocity (the surface friction within the surface layer). The azimuthal velocity in Eq. (10) should be written as $\langle u_x \cos\lambda + u_y \sin\lambda \rangle$ in the Cartesian coordinates, where u_x and u_y are the velocities in x and y direction, respectively (e.g., Persing et al., 2013). The friction velocity is also expressed as $C_D\sqrt{u^2+v^2}$ with C_D being the drag coefficient, which is equivalent to $C_D\sqrt{u_x^2+u_y^2}$ in the Cartesian coordinates. It follows, therefore, that in the absence of net flux through the lateral boundary of a tropical cyclone, Eq. (8) is rewritten as

$$\frac{d\hat{M}_r}{dt} = \int_0^R \rho_H r^2 \langle \tau_{zH} \rangle dr - \int_0^R \rho_s r^2 \langle u_*^2 \rangle dr, \tag{11}$$

In general, the vertical momentum flux in a tropical cyclone is dominated from the bottom, particularly during the developing stage. This suggests that Eq. (11) may be rewritten as

$$\frac{d\hat{M}_r}{dt} = -\int_0^R \rho_s r^2 \langle u_*^2 \rangle dr. \tag{12}$$

Since the right hand side of Eq. (12) is obviously negative-valued, the TRAM of a tropical cyclone in the developing and mature stages should decrease monotonically with time. The loss of angular momentum in the course of development, as represented in Eq. (12), is a direct consequence of the contrast in boundary conditions between the top and surface of a tropical cyclone whose radial-vertical circulation is driven by heating over the central region; in the upper layer where anti-cyclonic flow is formed, almost non-viscous motion tends to conserve the angular momentum, whereas this is not the case in the lower layer where cyclonic flow is maintained (Emanuel, 2003; Kwon and Cheong, 2010; Cheong et al., 2011; Hakim, 2011). Interestingly, a completely opposite tendency is found for the circulations driven by cooling (rather than heating) over the central region. In such a situation, anticyclonic and cyclonic circulations are established in the lower and upper layers, respectively (e.g., Hignett et al., 1981; Read, 1986; Kimura et al., 1992).

In the decaying stage, the first term in Eq. (11), the upper-boundary momentum flux, is no longer negligible and starts to play a role in weakening the anticyclonic flow aloft. The surface momentum flux, however, continues to diminish TRAM. As a result, the tendency of TRAM may remain negative in the early period of the decaying stage. The impact of the surface momentum flux is much stronger than that of the upper momentum flux due to strong shear near the surface, which will eventually terminate the dominance of the surface momentum flux over the upper momentum flux. This would lead to the dominance of the first term on the right hand side of Eq. (11), i.e., the upper momentum flux, over the second term, resulting in a positive tendency or increase in TRAM. It should be remembered that since this tendency is considerably small, the recovery process for the lost TRAM will take a relatively long time.

The development of a tropical cyclone is maintained by condensational heating of water-vapor supplied from the sea surface (Tuleya and Kurihara, 1974; Anthes, 1982; Emanuel, 2003; Cheong et al., 2011). However, it is known that such a thermal forcing does not explicitly appear in the angular momentum equation of (4) because it is directly related to the radial-vertical circulation. If the thermal forcing is removed, the tropical cyclone will enter the decaying process and the radial-vertical circulation as well as the tangential wind (both in the lower and upper layers) are expected to weaken monotonically with time. In other words, the tropical cyclone

never experiences an increase in cyclonic rotation (i.e., tangential wind) in the decaying stage if the decaying process commences due to the removal of the forcing from condensation heating. In this regard, the time evolution of TRAM, accompanied by monotonic decreases in both upper-layer cyclonic and lower-layer anticyclonic rotations in the decaying stage, differs fundamentally from the spin-down processes that are used to explain the decaying process of the vortices at the tropical cyclone-scale (Montgomery et al., 2001) in a quasi-gradient wind balance or large-scale in quasi-geostrophic wind balance (Holton and Hakim, 2012). The spin-down process therein gives rise to the radial circulations due to surface friction, which in turn contributes to an increase in the tangential wind as well as a widening of the vortex above the planetary boundary layer (PBL). However, this kind of ideal process is not likely to occur in decaying tropical cyclones (Anthes, 1982; Pielke, 1984; Cotton and Anthes, 1989). This issue will be addressed more using numerical simulations in the following section.

3. Numerical experiments

The life cycle of a tropical cyclone is simulated using the WRF-model version 3.4.1 (Skamarock et al., 2008) under the initial condition of an ideal axisymmetric tropical cyclone. Model options and parameters are depicted in Table 1. Domain size is set as large as 6,000 km × 6,000 km in order to appropriately represent the weak-wind outer region of the tropical cyclone, and the open boundary conditions for the lateral boundary conditions are applied to prevent the reflection of gravity waves. With the large computational domain, the influence of the lateral boundaries can be minimized. The model top is given as 10 hPa, which seems to be sufficient to adequately reproduce tropical cyclones. Two kinds of axisymmetric tropical cyclone (or vortices), one from Chan and Williams (1987) (hereafter type I vortex) and the other from Kwon and Cheong (2010) and Cheong et al. (2011) (hereafter type II vortex), are used, which in many respects are

Table 1. Weather Research and Forecasting (WRF; v3.4.1) model options used for the simulation of tropical cyclones with idealized initial vortices of axisymmetry.

Resolution	12 km × 12 km
Domain size	6,000 km × 6,000 km
Number of vertical layers	35
Uppermost layer of the model	10 hPa
PBL parameterization	YSU scheme (Hong et al., 2006)
Cumulus parameterization	Kain-Fritsch scheme (Kain and Fritsch, 1990)
Microphysics	WSM6 (Hong and Lim, 2006)

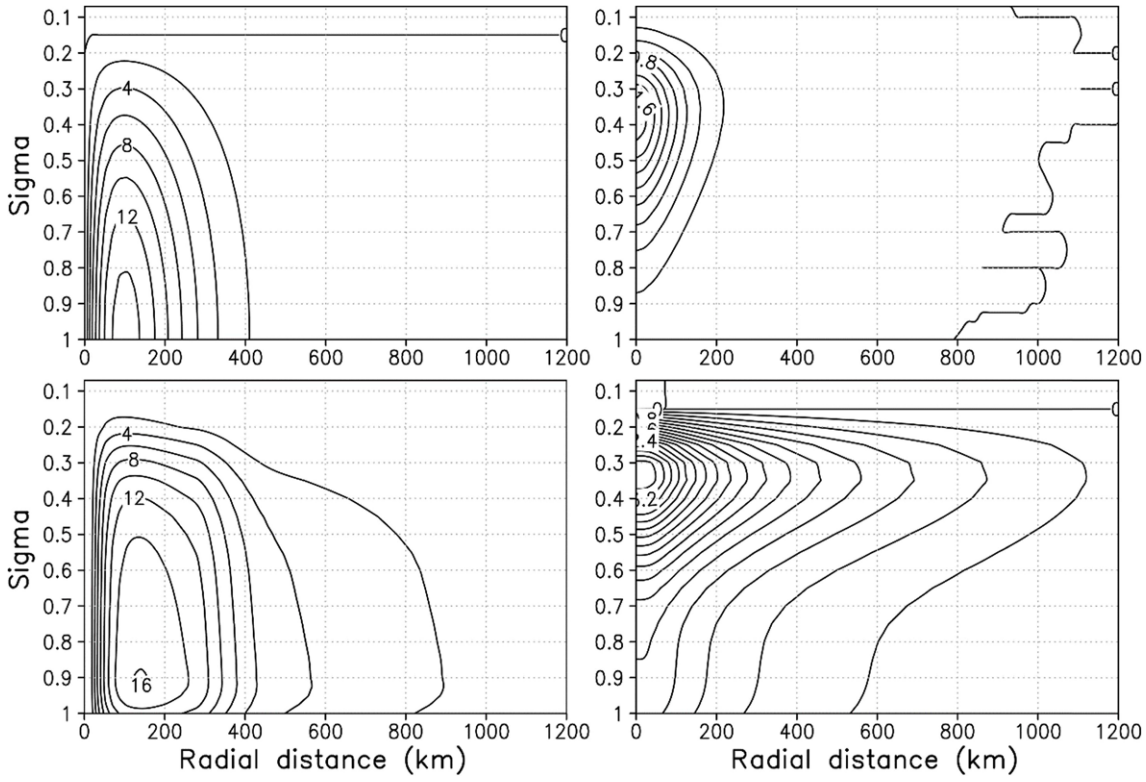

Fig. 1. Radial-vertical distribution of tangential wind (left column) and temperature perturbation (right column) of initial vortices, for type I (upper panels) and type II (lower panels). Contour intervals are 2.0 m s^{-1} and 0.2 K, respectively.

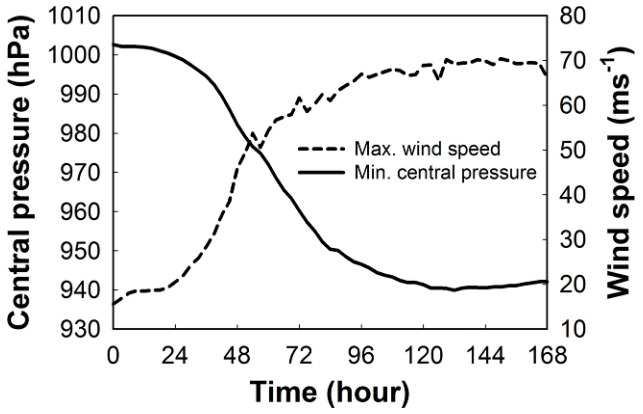

Fig. 2. Time variation of the minimum central pressure and the maximum tangential wind of the type I vortex during the initial 7 days of simulation.

reminiscent of developing tropical cyclones (Fig. 1). The former has narrow cyclonic winds whereas the latter gives wider and higher cyclonic winds in the troposphere; both cyclones have a quiescent upper layer (that is, the upper-layer anticyclonic flow was removed for better comparison). Unlike type I, type II has a realistic boundary layer structure. A gradient-wind balance among the pressure gradient force, the Coriolis force, and the centrifugal force is common to these vortices (Cotton and Anthes, 1989; Holton and Hakim, 2012; Chen et al., 2014; Miyamoto et al., 2014; Nguyen and Chen, 2014). For simplicity, the Coriolis parameter is given a constant value of 20°N, which allows the tropical cyclone to remain at its initial position. With this, the vortex tends to remain in an axisymmetric structure throughout the simulation period (Montgomery et al., 2001; Leonov, 2014).

Figure 2 presents the time variation of minimum central pressure (p_c) and maximum tangential wind (v_{max}) for 7 days. The central pressure is seen to diminish steadily with time, whereas the tangential wind intensifies monotonically with time, which is indicative of a developing tropical cyclone. At around 36 h, the time-change rate of minimum pressure begins to increase sharply until around 72 h, with an approximate average of –2.3 hPa h^{-1}. This is followed by a nearly steady state (cf. Hakim, 2011) beyond that. The surface pressure, horizontal wind vectors at the 900 hPa level, azimuthally-averaged tangential wind, and azimuthally-averaged radial wind are illustrated in Fig. 3 to demonstrate a well-established tropical cyclone that is nearly axisymmetric. It was found that the magnitude of the asymmetric component is tens of thousands times smaller than that of the symmetric component.

Shown in Fig. 4 is the time evolution of TRAM calculated for various radii of volume integration with a fixed value of $H = 12$ km. It is clear from the figure that TRAM decreases with time for all radii of integration regardless of initial vortex specification. The characteristics of time variation in TRAM appear to correspond well with those of p_c and v_{max}, as is evident from the rather sharp decrease with time at around 36 h. It is worth noting that the spinning-up, i.e., the intensifying cyclonic swirling flow, is accompanied by a decrease in TRAM. In the case of the type I vortex, TRAM is positive in the initial stage but becomes negative around 70 h for $R =$ 2,000 km. The results suggest that the circulation system of a developed tropical cyclone may be regarded as an anti-cyclonic rotation, which is consistent with both the conceptual model and the numerical simulations (Emanuel, 2003; Hakim, 2011; Smith et al., 2014). In such a system, the tangential velocity in the cyclonic-flow region is much weaker than what would be achieved in the absence of surface friction. In the case of the type II vortex, the TRAM for $R = 2{,}000$ km was significantly decreased but retained a positive sign until the end of the simulation period. This is attributed to the larger size of the type II vortex; that is, the much larger initial amount of TRAM. As can be seen in Fig. 4, the initial TRAM at $R = 2{,}000$ km for the type II vortex was about one order of magnitude larger than that of the type I vortex.

A decrease in TRAM with time is a dynamical consequence of bottom friction, which causes the tropical cyclone to lose angular momentum. As given by Eq. (8), the loss of TRAM can be explained by the combined effect of the torque associated with the radial-advective momentum flux and the frictional momentum flux at the surface and the top. To confirm this, the time-change rate of TRAM and the torques N_z and N_r are calculated separately from the gridpoint data at every time step (Fig. 5). We then apply a moving average with a 12 h interval to the time series. As is consistent with the time variation (as in Fig. 4), the time change rate of TRAM retains a negative value, which, as expected, appears to match well with the torques. As it should be, the frictional torque is found to be negative throughout the integration period, whereas the radial-advective momentum flux is maintained positive, except for a few-hours period before 60 h in the developing stage. The tropical cyclone receives the RAM through the lateral boundary and loses the RAM to the surface. It loses more RAM than it gains from the environment through the lateral boundary. These features, which are found for the time-variation of the RAM, are common to type I and type II vortices.

As shown in Fig. 4, the characteristics of the decreasing tendency of the TRAM are more conspicuous as the radius of the volume integration becomes larger. For a sufficiently large radius, the time-change rate of RAM is expected to be solely determined by the surface frictional torque, as given by Eqs. (11) and (12). Figure 6 is presented to address this point by changing the radius of the volume integration from $R =$ 1,000 km to $R = 2{,}000$ km for the same simulations shown in Fig. 5. The difference between the time tendency of TRAM and the frictional torque is found to be larger for a smaller radius but smaller for an increased radius. For the largest radius of the four cases, i.e., $R = 2{,}000$ km, the two curves appear to run in almost the same fashion with a relatively narrow gap. The difference between the two is estimated to be only 10% after approximately 120 h.

Numerical simulations shown above are focused on a short

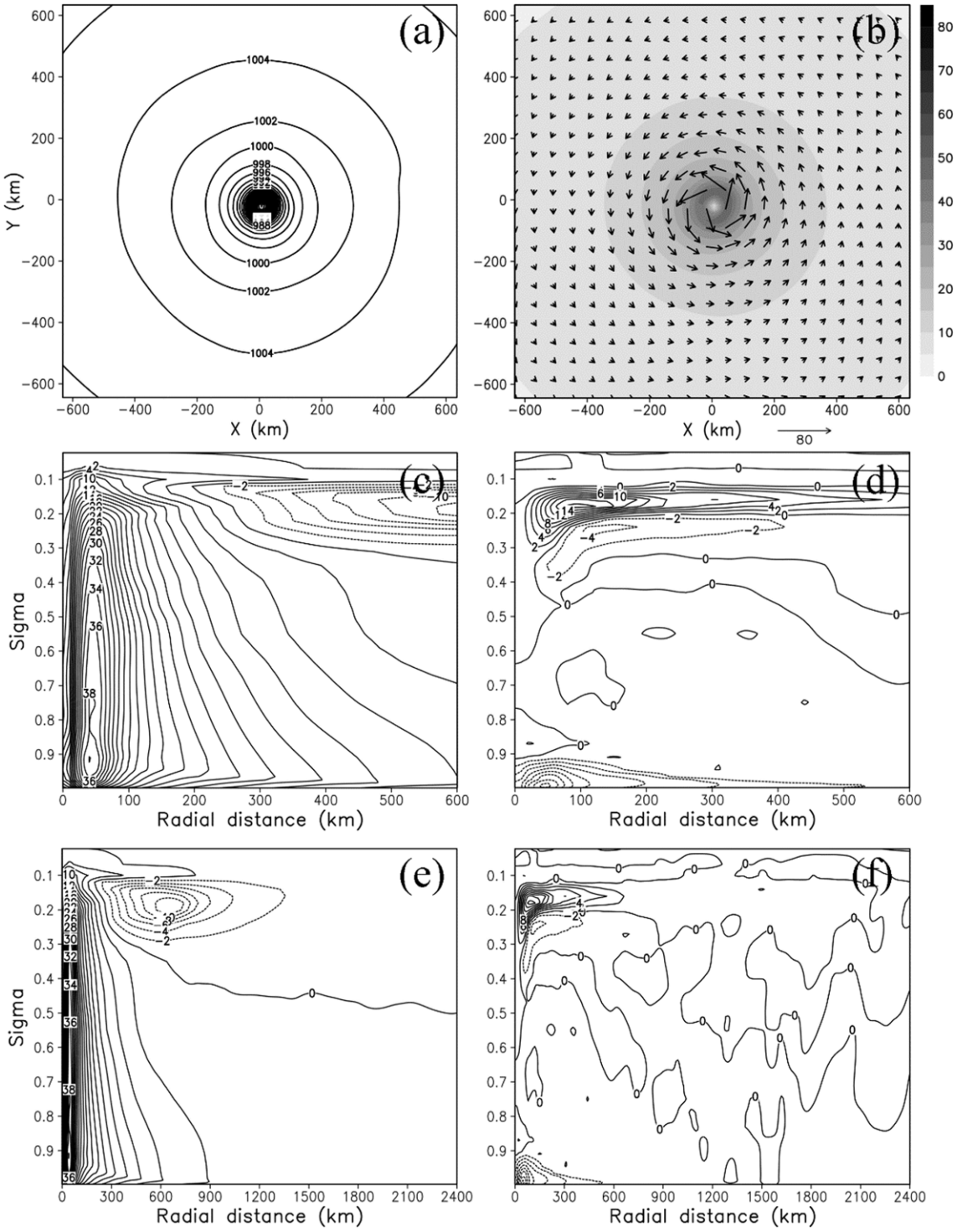

Fig. 3. Distribution of the surface pressure (a), horizontal wind vectors at the 900 hPa level (b), axisymmetric tangential wind (c), and axisymmetric radial wind (d) of the type I vortex at 72 h. Plots of (e) and (f) are the same as (c) and (d), respectively, except for an increased radial-range. Contour intervals for the surface pressure and the velocity are 2 hPa and 2 m s^{-1}, respectively.

term behavior of the tropical cyclones, over a period of a typical lifetime. Longer period simulations are expected to show almost the same results of angular momentum loss as above except for a sustained decrease of the TRAM even though an approximate steady-state, in terms of the minimum central pressure and the maximum wind, has been reached

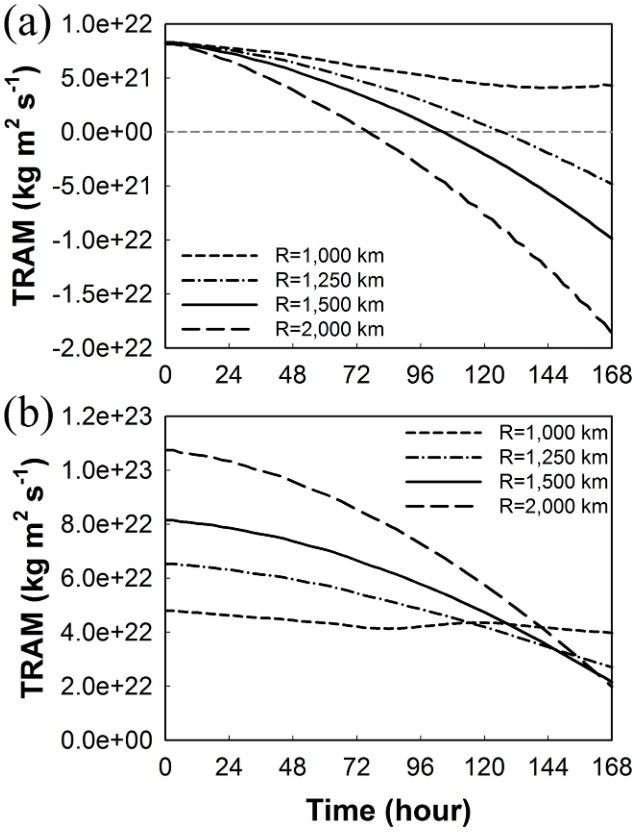

Fig. 4. Time variation of total relative angular momentum (TRAM; $\hat{M}_r$) for various radial extents of volume integration: initial tropical cyclones of type I (a) and type II (b).

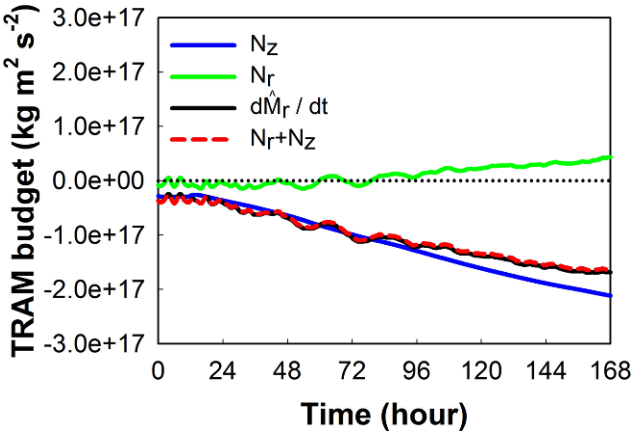

Fig. 5. Time evolution of the time-change rate of TRAM ($d\hat{M}_r/dt$; black line), N_r (green line), N_z (blue line), and $N_r + N_z$ (dashed red line) for the type I vortex, where $N_z = N_{zH}+N_{zB}$. The volume integration was carried out for the cylindrical column of H = 12 km and R = 1,500 km. The time-change rate (black line) was produced by approximation of the time derivative using the centered finite difference method with grid point data at every time step. A moving average with a 12-h interval was applied to the time series.

over this period. Such a sustained decrease of the TRAM in the case of long term simulation is believed to be caused by the ideal model setting such as sustained SST forcing, exclusion of other atmospheric motions, and removal of spherical geometry (or beta effect). However, even in the simulation over an extended period, the TRAM will reach an asymptotically-steady state superimposed by a certain amplitude of oscillation around its statistical average state. If the long term simulations are carried out, it may be necessary to set the SST forcing as well as SST cooling outside the tropical cyclone. This will bring about a statistical steady state in rather a shorter period and contribute to preventing an unrealistically large size of the tropical cyclone.

Dominance of the anti-cyclonic (or cyclonic) rotation as a whole in the tropical cyclone system, termed sub-rotation or negative super-rotation (Read, 1986; Lim et al., 2009), can be represented with a quantitative measure, termed the super-rotation ratio, which is defined as the ratio of TRAM to TPAM [refer to Eq. (6)]:

$$\Gamma_{rot}(t) \equiv \frac{I_\omega \omega}{I_\omega \Omega} = \frac{\hat{M}_r(r)}{\hat{M}_\Omega(r)}, \tag{13}$$

where I_ω denotes moment of inertia, ω is the angular velocity that the tropical cyclone would possess if it were in a solid-body rotation. When Γ_{rot} is positive (negative), it is referred to as a super-rotation (sub-rotation), which is used to describe the phenomenon where the whole rotating motion is in the same (opposite) direction as the rotation of the Earth (Read, 1986; Kimura et al., 1992; Lim et al., 2009). Figure 7 illustrates how the super-rotation ratio varies with time for the cases where R = 1,500 km and R = 2,000 km. The super-rotation ratio decreases with time, as can be expected from Fig. 4, reaching minimum values of 0.0011 (–0.00019) around 84 h and –0.0047 (–0.0029) by 168 h for R = 1,500 km (R = 2,000 km).

To observe the time variation in TRAM of well spun-up (or developed) vortices and the associated frictional torque in the absence of the SST forcing, the SST was lowered linearly (switched off) from 26.5°C to 21°C between 120 h and 126 h. The time variation of the minimum central pressure in this simulation is provided in Fig. 8. As it should be, the minimum central pressure shows a gradual increase to the initial value soon after switching off the SST forcing. Similarly, the tendency of the TRAM of the tropical cyclone has also increased after the SST is reduced, as presented in Fig. 9; however, the TRAM maintains a negative sign, meaning that the tropical cyclone is still losing the angular momentum. Interestingly, even after switching off the SST forcing, the radial-momentum flux (N_r), having positive values, continued to increase the TRAM for a few hours, whereas the frictional momentum flux (N_z) has turned into increasing phase from decreasing phase. Note that the initial TRAM may not be fully recovered even though the period of simulation is extended, but the time tendency of the TRAM will increase continuously and will ultimately restore its initial value because the upper-layer anticyclonic rotation, which is likely to be the major contributing factor in this period, dissipates gradually down.

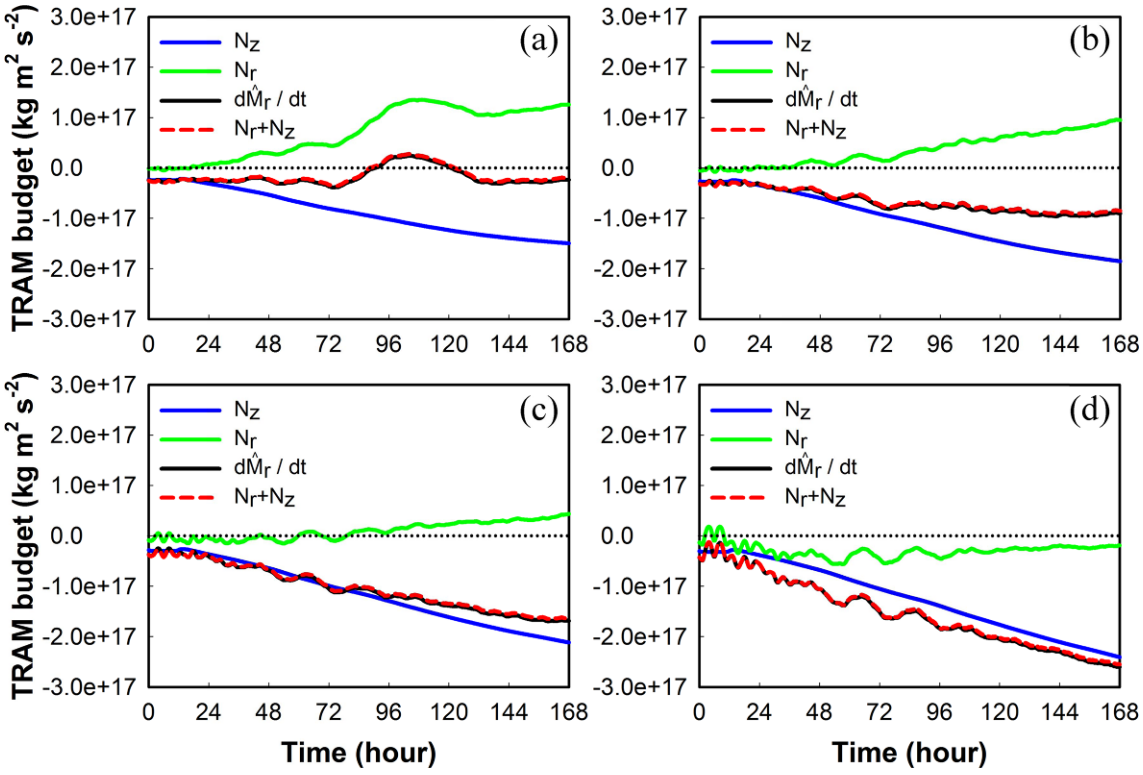

Fig. 6. Time evolution of the time-change rate of TRAM ($d\hat{M}_r/dt$; black line), N_r (green line), N_z (blue line), and $N_r + N_z$ (dashed red line) for the radii of volume integration of R = 1,000 km (a), R = 1,250 km (b), R = 1,500 km (c), and R = 2,000 km (d) for the type I vortex, where $N_z = N_{zH} + N_{zB}$. The time-change rate (black line) was produced in the same way as in Fig. 5.

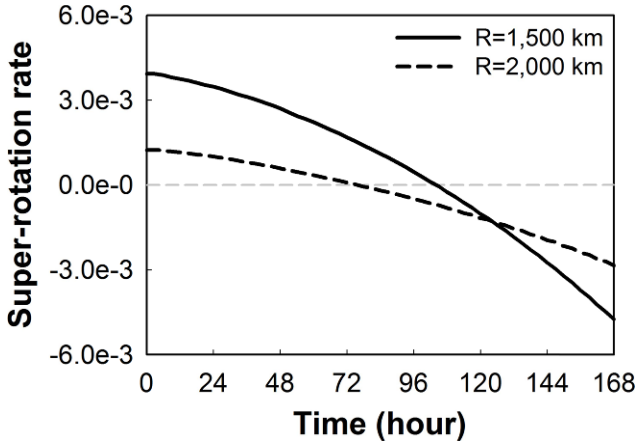

Fig. 7. Time variation of the super-rotation ratio defined by Eq. (13) for the radii of volume integration of R = 1,500 km (solid line) and R = 2,000 km (dashed line) for the type I vortex.

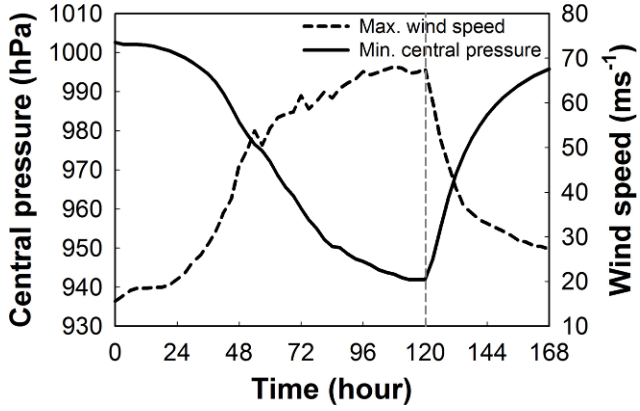

Fig. 8. Same as in Fig. 2 except that SST forcing was removed at 120 h, as indicated by the vertical dashed gray line.

4. Summary and concluding remarks

In this study, angular momentum was analyzed for an axisymmetric tropical cyclone in the context of *f*-plane approximation with a focus on the volume integrated quantity. The angular momentum budget analysis in the cylindrical coordinates was shown to be formulated in a simple relationship between the TRAM and the torque: The TRAM is subject to time change only by the boundary fluxes represented with the radial-advective flux and the vertical frictional flux. Numerical simulations using WRF v3.4.1 were carried out to confirm the TRAM budget analysis for the axisymmetric tropical cyclone. Two kinds of axisymmetric vortex without anticyclonic rotation in the upper layer were incorporated as

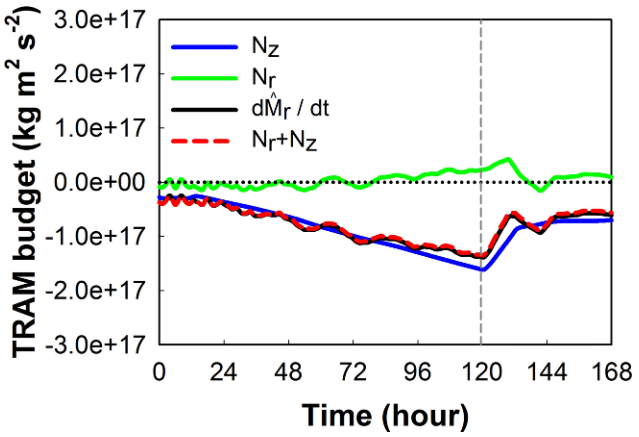

Fig. 9. Same as in Fig. 5 except that SST forcing was removed at 120 h, as indicated by the vertical dashed gray line.

initial conditions. The results are summarized as follows.

- The TRAM of an axisymmetric tropical cyclone decreases with time in the developing stage because of the frictional loss of angular momentum near the surface. The decrease in TRAM becomes larger when the radius for budget analysis of the angular momentum is set larger.
- If the SST forcing is removed in the mature stage, the tropical cyclone starts to decay gradually. Even in this case, however, the tropical cyclone continues to lose the angular momentum. While the angular momentum loss rate over time diminishes slowly in the course of development, the loss rate changes rather sharply by the SST forcing removal.
- Angular momentum decrease was represented with the super-rotation index, the ratio of TRAM to the planetary angular momentum. Typically, it was less than zero, meaning a sub-rotation, for the tropical cyclones simulated in this study, and found to be only a few tenth percent even at the time of full development.

The inclusion of spherical geometry, which is more realistic than the cases dealt with in the present study, would, in many ways, result in quite different TRAM behavior due to the beta-drift of the tropical cyclone, the waves generated by the tropical cyclone, and interaction between the waves and the tropical cyclone. However, on average, during its lifetime, a tropical cyclone is expected to undergo a decrease in TRAM with time, although it temporarily experiences an increase in TRAM due to its associated waves.

Acknowledgments. This research was supported by Korea Meteorological Industry Promotion Agency (KMIPA 2015-5130). Hyun-Gyu Kang acknowledges the financially support, through the post-doctoral fellow program, by the BK21 Plus Project of the Graduate School of Earth Environmental Hazard System. This study was motivated from the discussion with Professor Ryuji Kimura on the superrotation of the Venus atmosphere and the winter cold-air outbreak model. Hyeong-Bin Cheong would like to thank Ryuji Kimura, an emeritus Professor of the University of Tokyo, for helping him have insight on and continuing interest in such a topic. The authors would like to appreciate the anonymous reviewers for useful comments.

Edited by: Soon-Il An

References

Anthes, R. A., 1982: *Tropical Cyclones: Their Evolution, Structure and Effects*. American Meteorological Society, 208 pp.

Bird, R. B., W. E. Stewart, and E. N. Lightfoot, 2007: *Transport Phenomena, Revised second Edition*. John Wiley & Sons, Inc., 905 pp.

Chan, J. C. L., and R. T. Williams, 1987: Analytical and numerical studies of the beta-effect in tropical cyclone motion. Part I: Zero mean flow. *J. Atmos. Sci.*, **44**, 1257-1265.

Cheong, H.-B., I.-H. Kwon, H.-G. Kang, J.-R. Park, H.-J. Han, and J.-J. Kim, 2011: Tropical cyclone track and intensity prediction with a structure adjustable balanced vortex. *Asia-Pac. J. Atmos. Sci.*, **47**, 293-303, doi:10.1007/s13143-011-0018-7.

Chen, C.-Y., Y.-L. Chen, and H. V. Nguyen, 2014: The spin-up process of a cyclone vortex in a tropical cyclone initialization scheme and its impact on the initial TC structure. *Sci. Online Lett. Atmos.*, **10**, 93-97, doi: 10.2151/sola.2014-019.

Cotton, W. R., and R. A. Anthes, 1989: *Storm and Cloud Dynamics*. Academic press, 833 pp.

Emanuel, K., 2003: Tropical cyclones. *Annu. Rev. Earth Pl. Sci.*, **31**, 75-104.

Hakim, G. J., 2011: The mean state of axisymmetric hurricanes in statistical equilibrium. *J. Atmos. Sci.*, **68**, 1364-1376, doi:10.1175/2010-JAS3644.1.

Holland, G. J., 1983: Angular momentum transport in tropical cyclones. *Quart. J. Roy. Meteor. Soc.*, **109**, 187-209.

Hignett, P., A. Ibbetson, and P. D. Killworth, 1981: On rotating thermal convection driven by nonuniform heating from below. *J. Fluid Mech.*, **109**, 161-187.

Holton, J. R., and G. J. Hakim, 2012: *An Introduction to Dynamic Meteorology*. Academic press, 552 pp.

Hong, S.-Y., and J.-O. J. Lim, 2006: The WRF single-moment 6-class microphysics scheme (WSM6). *J. Korean Meteor. Soc.*, **42**, 129-151.

_____, Y. Noh, and J. Dudhia, 2006: A new vertical diffusion package with an explicit treatment of entrainment processes. *Mon. Wea. Rev.*, **134**, 2318-2341.

Kain, J. S., and J. M. Fritsch, 1990: A one-dimensional entraining/detraining plume model and its application in convective parameterization. *J. Atmos. Sci.*, **47**, 2784-2802.

Kimura, R.-J., N. Misawa, H.-B. Cheong, and A. Mori, 1992: Visualization by liquid crystal of circulation driven by local cooling in a rotating fluid layer. In *Atlas of Visualization, 1st Edition.* Visualization Soc of Japan Ed., Pergamon, 45-66.

Kwon, I.-H., and H.-B. Cheong, 2010: Tropical cyclone initialization with a spherical high-order filter and an idealized three-dimensional bogus vortex. *Mon. Wea. Rev.*, **138**, 1344-1367, doi:10.1175/2009MWR2943.1.

Leonov, A. I., 2014: Analytical models for hurricane. *Open J. Marine Sci.*, **4**, 194-213, doi:10.4236/ojms.2014.43019.

Lim, C. C., X. Ding, and J. Nebus, 2009: *Vortex Dynamics, Statistical Mechanics, and Planetary Atmosphere.* World Scientific Publishing Company, 224 pp.

Miyamoto, Y., M. Satoh, H. Tomita, K. Oouchi, Y. Yamada, C. Kodama, and J. Kinter III, 2014: Gradient wind balance in tropical cyclones in high-resolution global experiment. *Mon. Wea. Rev.*, **142**, 1908-1926, doi:10.1175/MWR-D-13-00115.1.

Montgomery, M. T., and R. K. Smith, 2017: Recent development in the

fluid dynamics of tropical cyclones. *Annu. Rev. Fluid Mech*., **49**, 541-574, doi:10.1146/annurev-fluid-010816-060022.

_____, H. D. Snell, and Z. Yang, 2001: Axisymmetric spindown dynamics of hurricane-like vortices. *J. Atmos. Sci*., **58**, 421-435.

_____, S. F. Abarca, and R. K. Smith, 2015: On the applicability of linear, axisymmetric dynamics in intensifying and mature cyclones. *Quart. J. Roy. Meteor. Soc.,* **5**, 1-11.

Nguyen, H. V., and Y.-L. Chen, 2014: Improvement to a tropical cyclone initialization scheme and impacts on forecast. *Mon. Wea. Rev.,* **142**, 4340-4356, doi:10.1175/MWR-D-13-00326.1.

Persing, J., M. T. Montgomery, J. C. McWilliams, and R. K. Smith, 2013: Asymmetric and axisymmetric dynamics of tropical cyclones. *Atmos. Chem. Phys.*, **13**, 12299-12341, doi:10.5194/acp-13-12299-2013.

Pielke, R. A., 1984: *Mesoscale Meteorological Modeling.* Academic press, 599 pp.

Read, P. L., 1986: Super-rotation and diffusion of axial angular momentum: I. 'Speed Limits' for axisymmetric flow in a rotating cylindrical fluid annulus. *Quart. J. Roy. Meteor. Soc*., **112**, 231-251, doi:10.1002/qj.49711247113.

Skamarock, W., and coauthors, 2008: A description of the advanced research Weather Research and Forecasting version 3. NCAR technical note NCAR/TN-475+STR, 113 pp.

Smith, R. K., M. T. Montgomery, and J. Persing, 2014: On steady-state tropical cyclones. *Quart. J. Roy. Meteor. Soc.*, **140**, 2638-2649, doi:10.1002/qj.2329.

Symon, K. R., 1971: *Mechanics, 3rd Edition*. Addison-Wesley, 639 pp.

Tuleya, R. E., and Y. Kurihara, 1974: The energy and angular momentum budgets of a three-dimensional tropical cyclone model. *J. Atmos. Sci*., **32**, 287-301.

Vogl, S., and R. K. Smith, 2009: Limitations of a linear model for the hurricane boundary layer. *Quart. J. Roy. Meteor. Soc.*, **135**, 839-850.